Electronic supporting information

Precise Construction of Pd Superstructures with Modulated Defect Properties for Solar-Driven Organic Transformation

Henglei Jia,*[a,‡] Jingzhao Li,[a,b‡] Fu-Kuo Chiang,[c,‡] Hao Wang,[d,e] Fan Li,[a] Zhong-Qing Lin,[f] Qifeng Ruan*[d,e] and Chun-yang Zhang*[b]

[a] College of Chemistry, Chemical Engineering and Materials Science, Shandong Normal University, Jinan 250014, China. E-mail: hljia@sdnu.edu.cn

[b] School of Chemistry and Chemical Engineering, Southeast University, Nanjing 211189, China. E-mail: zhangcy@seu.edu.cn

[c] National Institute of Clean-and-Low-Carbon Energy, Beijing 102209, China.

[d] Guangdong Provincial Key Laboratory of Semiconductor Optoelectronic Materials and Intelligent Photonic Systems, Harbin Institute of Technology, Shenzhen 518055, China. E-mail: ruanqifeng@hit.edu.cn

[e] Quantum Science Center of Guangdong-Hong Kong-Macao Greater Bay Area, Shenzhen-Hong Kong International Science and Technology Park, NO.3 Binglang Road, Futian District, Shenzhen 518055, China.

[f] Modern Experiment Technical Center, Anhui University, Hefei 230039, China.

* Corresponding author. E-mail: hljia@sdnu.edu.cn; ruanqifeng@hit.edu.cn; zhangcy@seu.edu.cn

‡ These authors contributed equally to this work.

Supporting Experimental Section

Chemicals. Pdlladium (II) acetylacetonate ($Pd(acac)_2$, 99.95%) and hexadecyltrimethylammonium bromide (CTAB, for molecular biology, ≥ 99.0%) were purchased from Sigma–Aldrich. Cetyltrimethylammonium chloride (CTAC, 99%), tungsten hexacarbonyl ($W(CO)_6$, 99.99%), *o*-phenylenediamine ($C_6H_8N_2$, 98%), and benzyl alcohol (C_7H_8O, 99%) were purchased from Macklin. Polyvinylpyrrolidone (PVP, molecular weight = 24000) and N,N-dimethylpropanamide (DMP, 98%) were purchased from Aladdin Reagent. Ethanol (C_2H_6O, 99%) and Acetone (C_3H_6O) were purchased from Sinopharm Chemical Reagent. 2,3-Diaminophenazine ($C_{12}H_{10}N_4$, 97%) was obtained from TCI. Deionized (DI) water with a resistivity of 18.2 MΩ·cm was used in all experiments.

Synthesis of the Pd SSs. In a typical preparation of Pd SSs, $Pd(acac)_2$ (50 mg), PVP (molecular weight = 29000, 160 mg), and CTAB (185 mg) were added into a mixture solution containing DMP (10 mL) and benzyl alcohol (2 mL) in a scintillation vial (20 mL). The resultant solution was stirred for about 1 h to obtain a yellow transparent solution. The scintillation vial was then transferred to an argon-filled glove box and $W(CO)_6$ (100 mg) was added into the above solution. The vial was capped and heated in an oil-bath (90 °C) for 25 min under magnetic stirring. The color of the solution was changed gradually from yellow to brown and finally black. The reaction solution was then cooled down to 0 °C in ice water. To obtain the Pd SSs, the reaction solution (3 mL) was added into acetone (7 mL) and the resultant solution was centrifugated once at 8500 rpm for 10 min. The precipitated product was redispersed in a mixture solution containing 3 mL of ethanol and 7 mL of acetone. The resultant solution was centrifugated once at 8000 rpm for 10 min and washed three times with ethanol/acetone (v/v: 3/7) mixture solution. The obtained Pd SSs was redispersed in anhydrous ethanol in a sealed scintillation vial, and can be stored in ambient conditions for six months. For further use, the Pd SS solution (3 mL) was added into acetone (7 mL), and the resultant solution was centrifugated at 8000 rpm for 10 min to collect the Pd SSs.

Synthesis of the Pd nano-tetrahedrons. The synthesis of Pd nano-tetrahedrons was similar to that of Pd SSs except that the amount of CTAB was changed as 0 mg.

Synthesis of the Pd nanosheets. The Pd nanosheets were prepared following a previously reported method with modifications.[1] Typically, $Pd(acac)_2$ (50 mg), PVP (molecular weight = 24000, 160 mg), and CTAB (185 mg) were added into a mixture solution containing DMP (10 mL) and DI water (2 mL) in a scintillation vial (20 mL). The resultant solution was stirred for about 1 h and $W(CO)_6$ (100 mg) was added under Ar atmosphere. The vial was capped and heated in an oil-bath (80 °C) for 30 min under magnetic stirring. The product was collected by centrifugation using ethanol/acetone mixture for several times.

Photocatalytic oxidation of OPDA. The photocatalytic oxidation reactions of OPDA were conducted in a customized glass reactor (100 mL) equipped with a quartz window on its top for light illumination. For a typical photocatalytic process, OPDA solution (0.005 M, 10 mL), Pd nanocrystal catalyst (0.055 mg/mL, 10 mL), and DI water (10 mL) were added into the reactor. The resultant solution was mixed by sonication for 30 s. A continuous Xe lamp (CEL-HXF 300 W) equipped with an AM 1.5G filter and a 420-nm cutoff filter (JB420) was used as the visible and NIR-light source. The optical power density was set at 100 mW cm^{-2}. The photocatalytic oxidation reactions of OPDA were carried out for 2.5 h. For each 30 min, 1 mL of the reaction solution was taken out and centrifuged to remove the catalyst. The yield of the obtained DAP in the supernatant was determined on an ultraviolet/visible/NIR spectrophotometer. Each photocatalytic experiment was repeated three times to calculate the average value and the standard deviation.

FDTD simulations. The scattering, absorption, and extinction spectra of Pd SSs were simulated using FDTD method.[2] The dielectric function of Pd was represented by fitting the data points of E. Palik. The Pd SSs were modeled as a tetrahedron-shaped Pd core and four legs on each tip. Each leg is built from four Pd nano-tetrahedrons, using average lengths measured from the TEM images. The refractive index of the surrounding water was set to be 1.33. An electromagnetic pulse was launched to simulate a propagating plane wave interacting with the Pd SSs. The scattering and absorption signals were then collected by energy monitors and normalized by the incident light power. The extinction spectra were calculated as the sum of scattering and

absorption. The electric field enhancement contours were recorded by a field profile monitor placed at a distance of 15 nm from the center of the Pd SSs.

Characterization. TEM imaging was conducted on an Talos L120C electron microscope operated at 120 kV. HRTEM, HAADF-STEM imaging, SAED, and EDX elemental mapping were carried out on a Thermo Fisher Talos F200S G2 microscopy. SEM images were taken on a ZEISS Sigma 300 microscopy. The extinction spectra were measured using a Hitachi U-3900 ultraviolet/visible/NIR spectrophotometer with 1.0 cm quartz cuvettes. XRD patterns were carried out on a Smart Lab Se diffractometer equipped with Cu Kα radiation. XPS spectra were obtained on a Thermo Scientific ESCALAB 250Xi spectrometer equipped with an Al Kα X-ray source (hν = 1486.6 eV). XAS measurements were performed at the beamline BL11B and BL14W1 in Shanghai Synchrotron Radiation Facility (SSRF), China. Inductively coupled plasma optical emission spectroscopy (ICP-OES) was measured on a Thermo Fisher iCAP PRO system. ^{1}H NMR spectra were measured on a Bruker Avance III 400M NMR spectrometer. LC–MS spectra were recorded on an Agilent 6530 Q-TOF LC/MS spectrometer.

Supplementary Figures

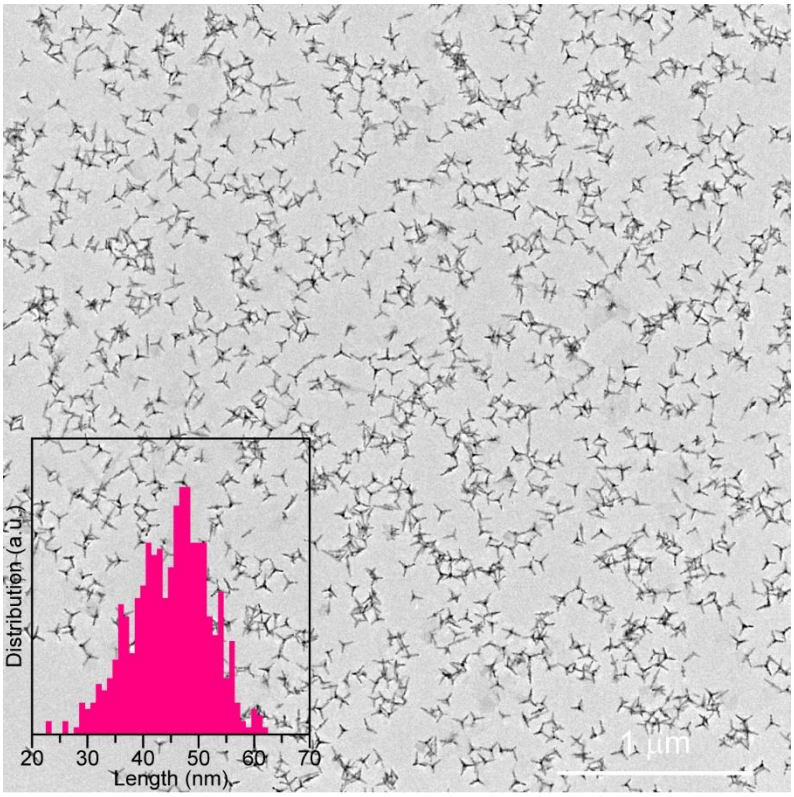

Fig. S1 Representative TEM image of the Pd SS-3 sample at a low magnification. The inset figure displays the leg length distribution of the Pd SSs.

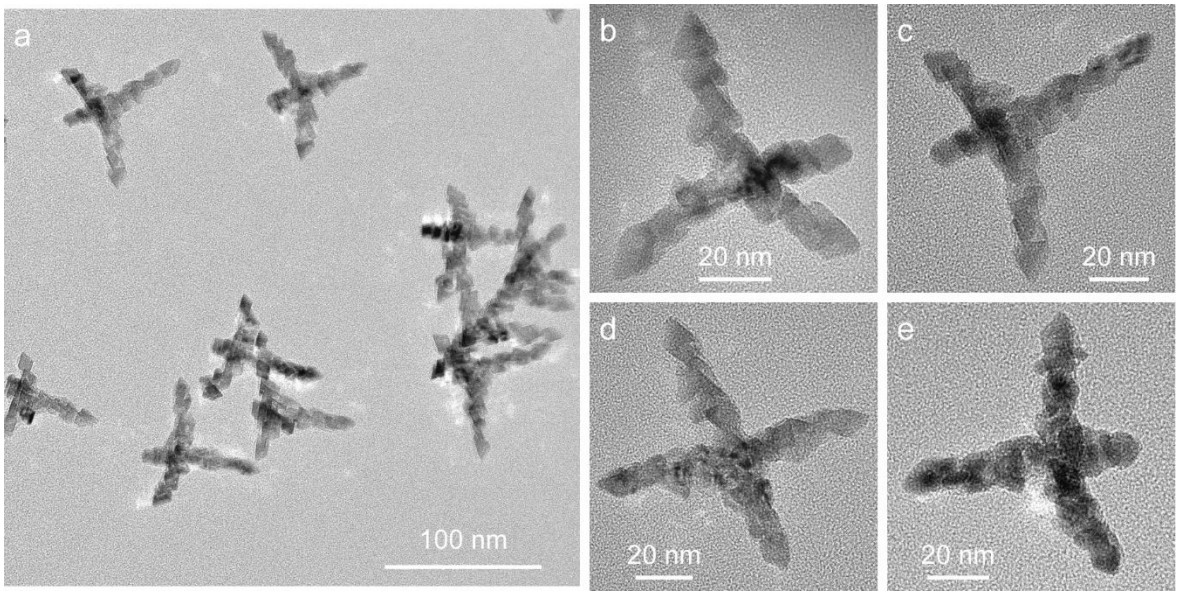

Fig. S2 Tilting TEM studies. Low-magnification (a) and representative single particle (b–e) TEM images of the Pd SSs after tilting 30°.

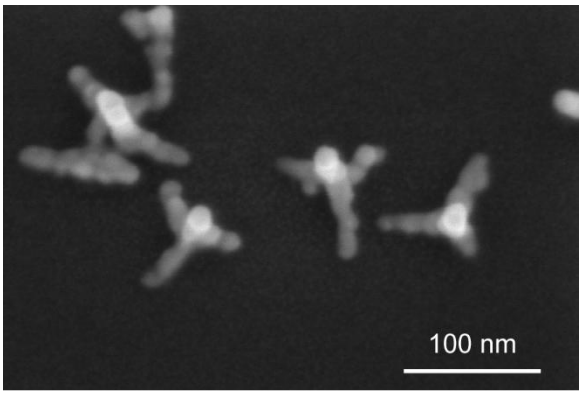

Fig. S3 High-resolution SEM image of the Pd SSs.

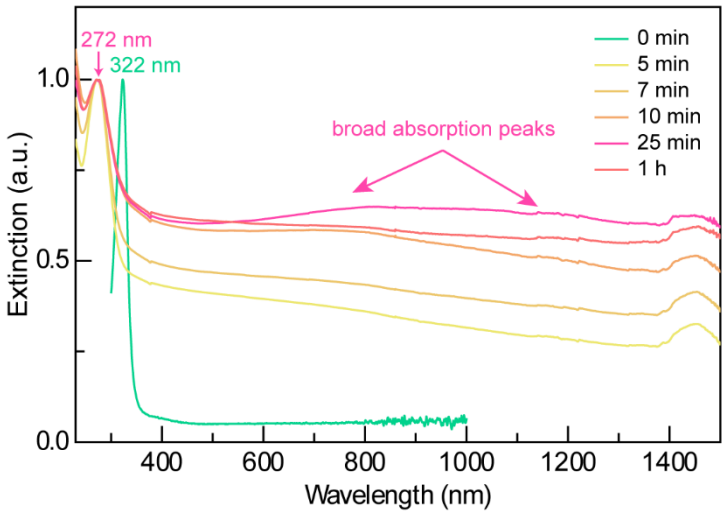

Fig. S4 Time-dependent extinction spectra of the reaction solution before and after the reaction.

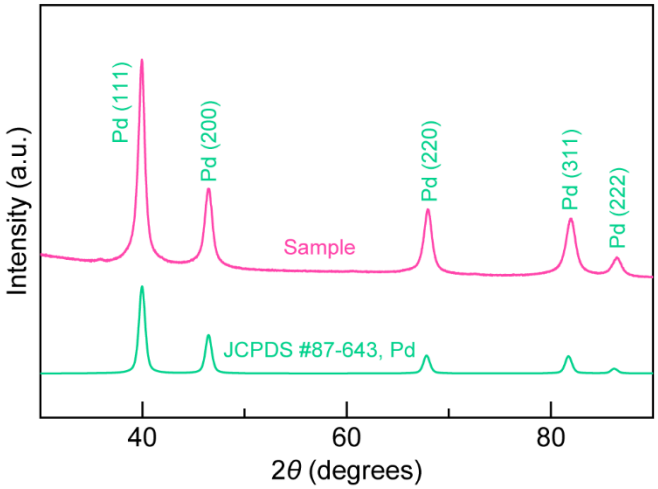

Fig. S5 XRD patterns of the Pd SS-3 sample. The red and green curves are the sample and the standard powder diffraction patterns of the face-centered-cubic structure of Pd (space group, F*m*-3*m*; lattice constant, 0.3908 nm), respectively.

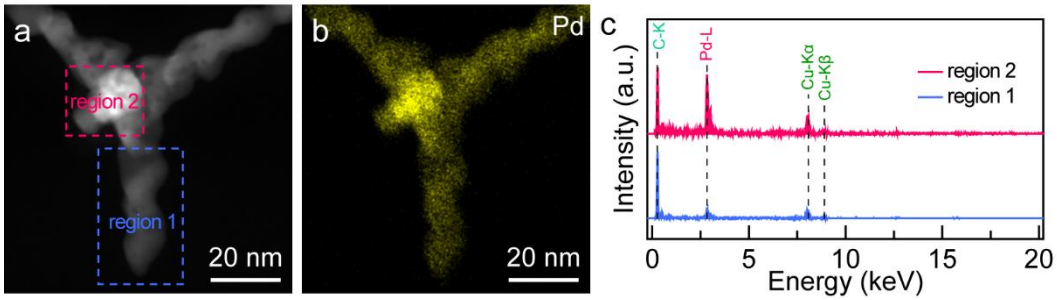

Fig. S6 EDX mapping results of Pd SS-3 after tilting 30°. (a–c) STEM (a), EDX map of Pd (b), and corresponding EDX spectra (c) taken from the two regions marked in (a).

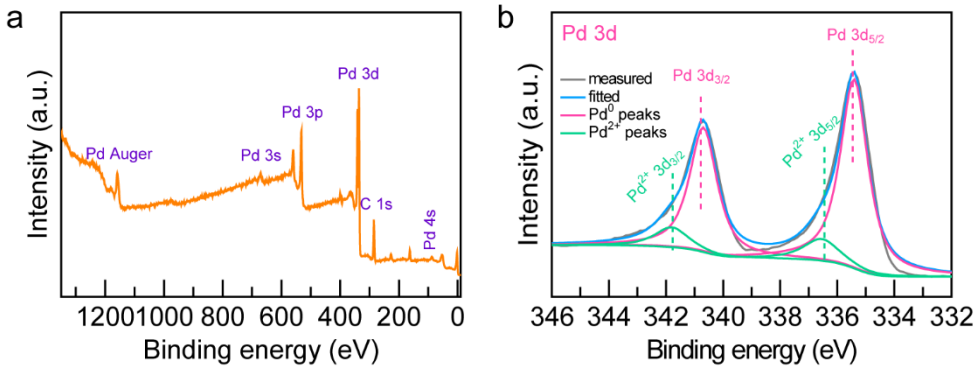

Fig. S7 XPS results of the Pd SS-3 sample. (a) Survey spectrum. (b) High-resolution spectra of Pd 3d.

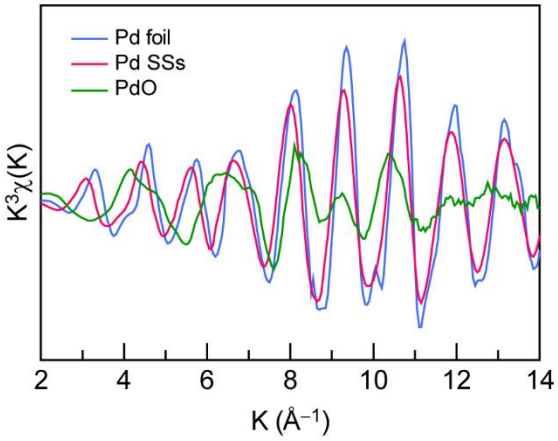

Fig. S8 Fourier transform spectra from EXAFS for Pd K-edge at *k* space.

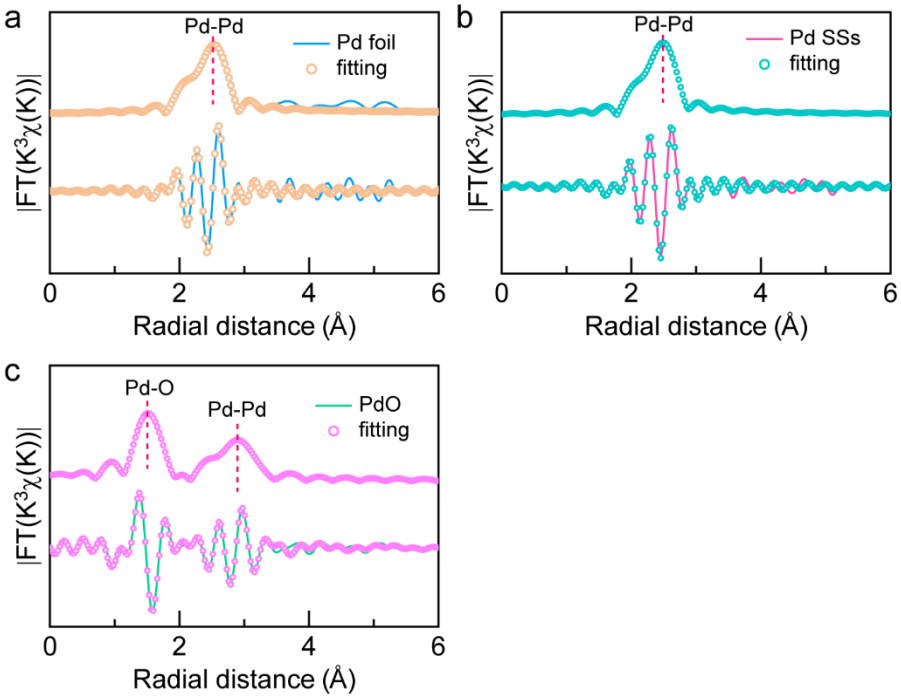

Fig. S9 Fitting results of EXAFS spectra at *R* space. (a–c) Fourier transform of Pd K-edge EXAFS fitting results of Au foil (a), Pd SS sample (b), and PdO (c), respectively.

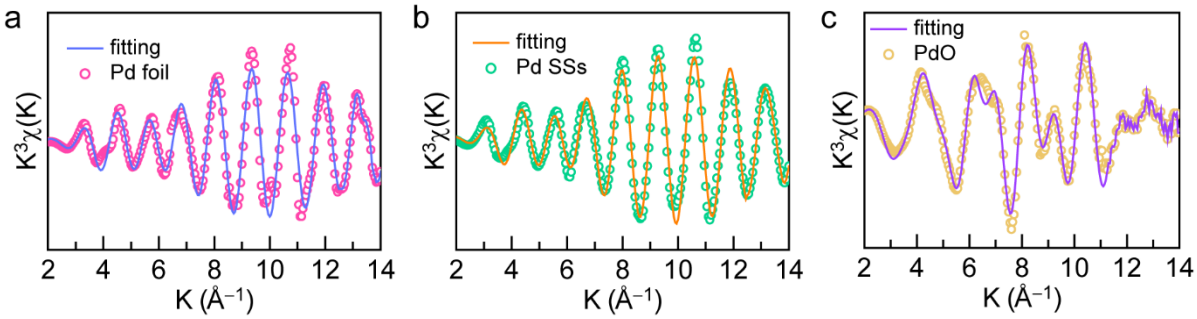

Fig. S10 Fitting results of EXAFS spectra at *k* space. (a–c) Fourier transform of Pd K-edge EXAFS fitting results of Pd foil (a), Pd SS sample (b), and PdO (c), respectively.

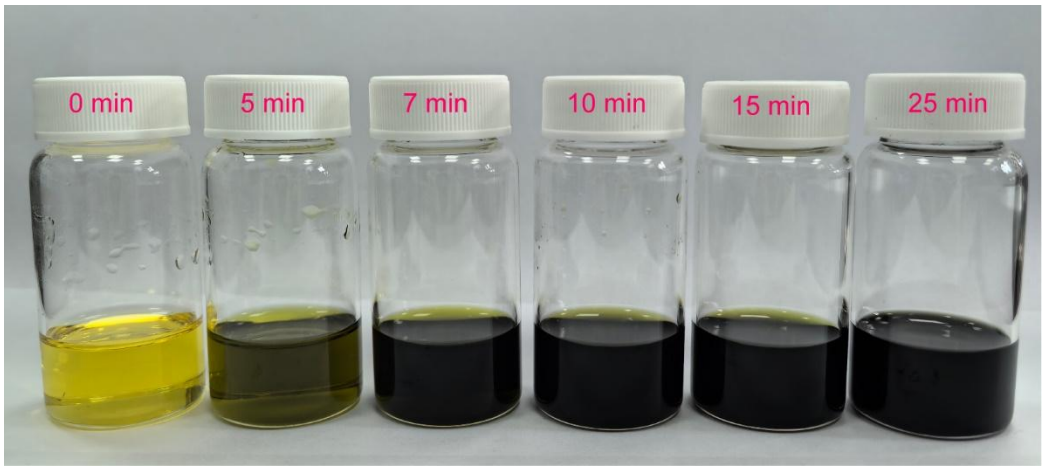

Fig. S11 Photograph of the reaction solutions at different reaction times.

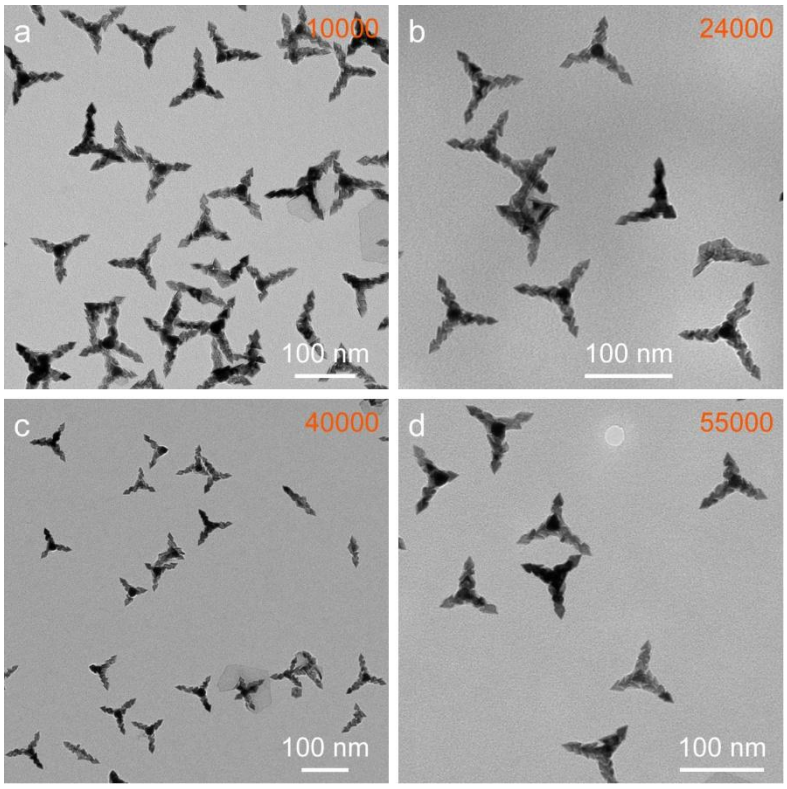

Fig. S12 Effect of the PVP molecular weight on the growth behaviour. (a–d) TEM images of the obtained Pd SSs growth with the PVPs with molecular weights of 10000 g mol^{-1} (a), 24000 g mol^{-1} (b), 40000 g mol^{-1} (c), and 55000 g mol^{-1} (d), respectively.

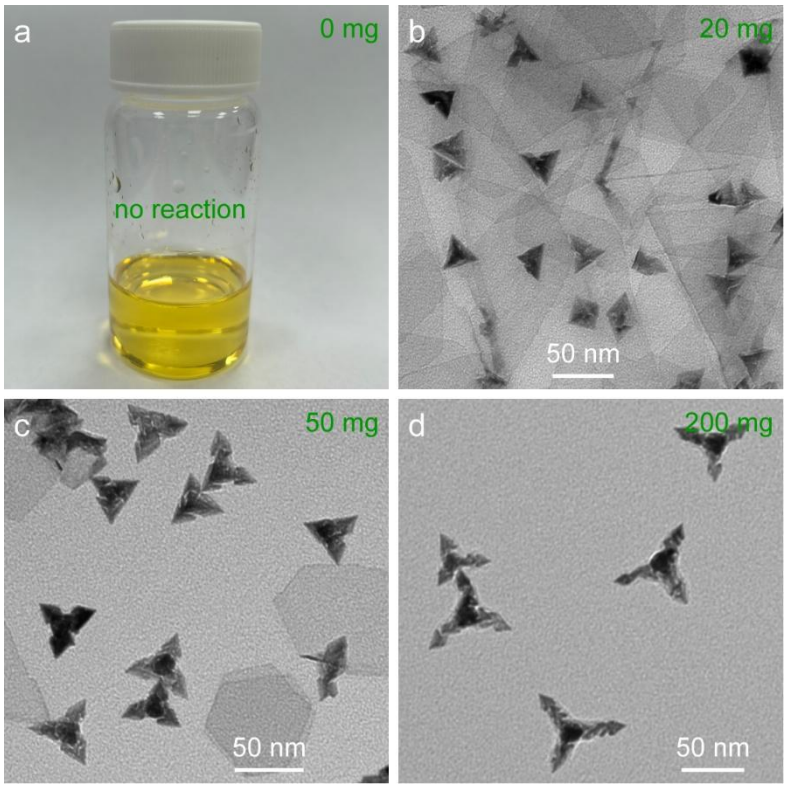

Fig. S13 Effect of the CO amount on the growth behaviour. (a) Photograph of the reaction solution without the addition of $W(CO)_6$. (b–d) TEM images of products when the addition amounts of $W(CO)_6$ are 20 mg (b), 50 mg (c), and 200 mg (d), respectively.

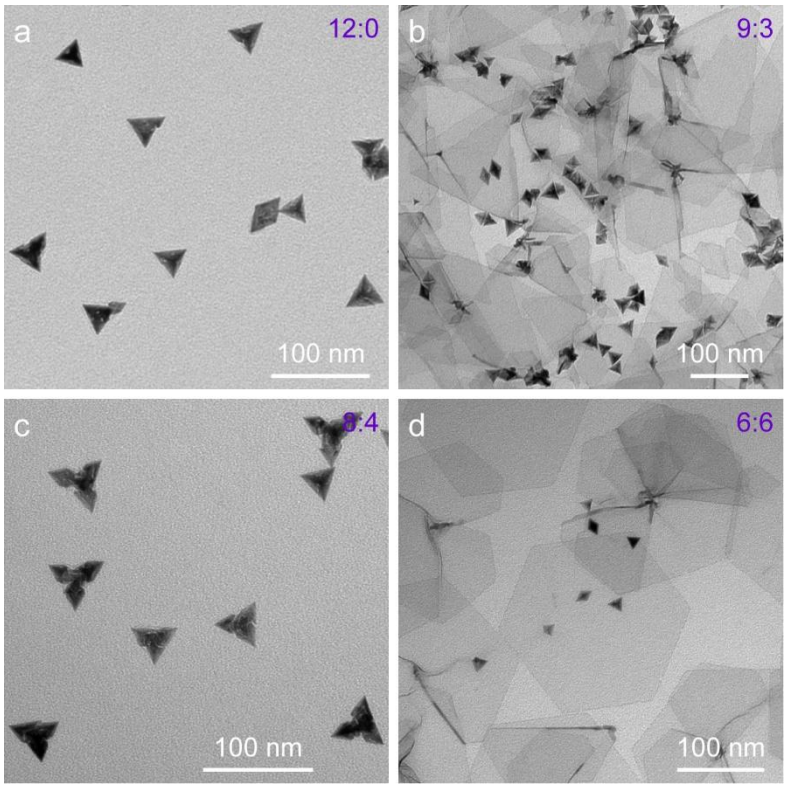

Fig. S14 Effect of the reducing capability of solvent on the growth behaviour. (a–d) TEM images of products when the volume ratios of DMF to benzyl alcohol are 12:0 (a), 9:3 (b), 8:4 (c) and 6:6 (d), respectively.

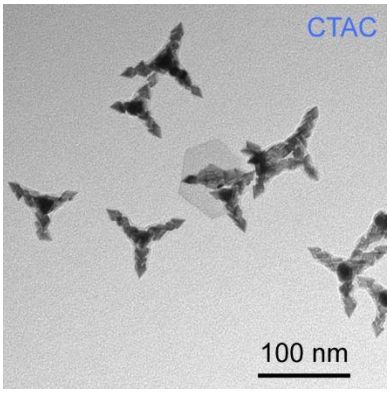

Fig. S15 Effect of the halide ion on the growth behaviour. TEM image of the obtained Pd SSs growth with CTAC rather than CTAB as the surfactant.

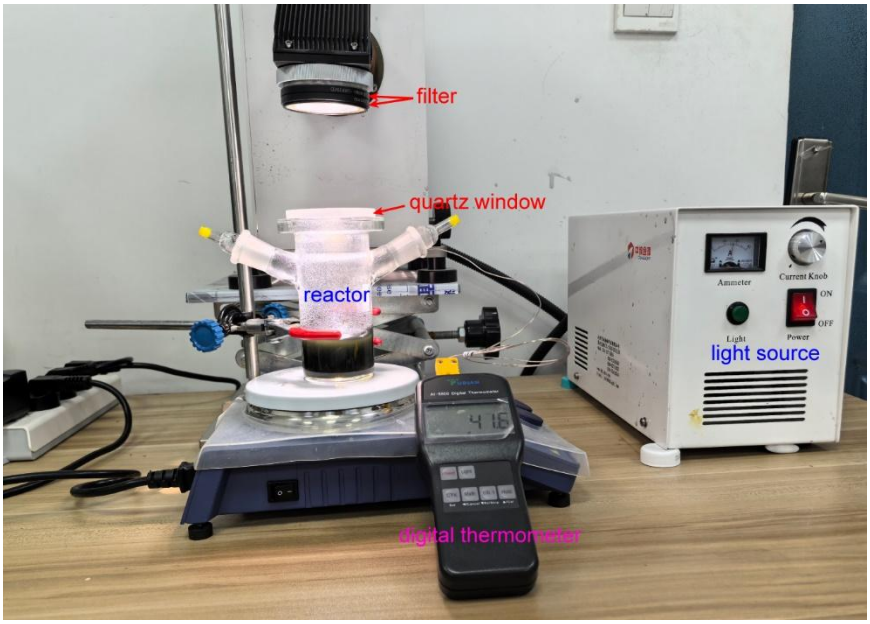

Fig. S16 Photograph of the photocatalytic system for OPDA oxidation.

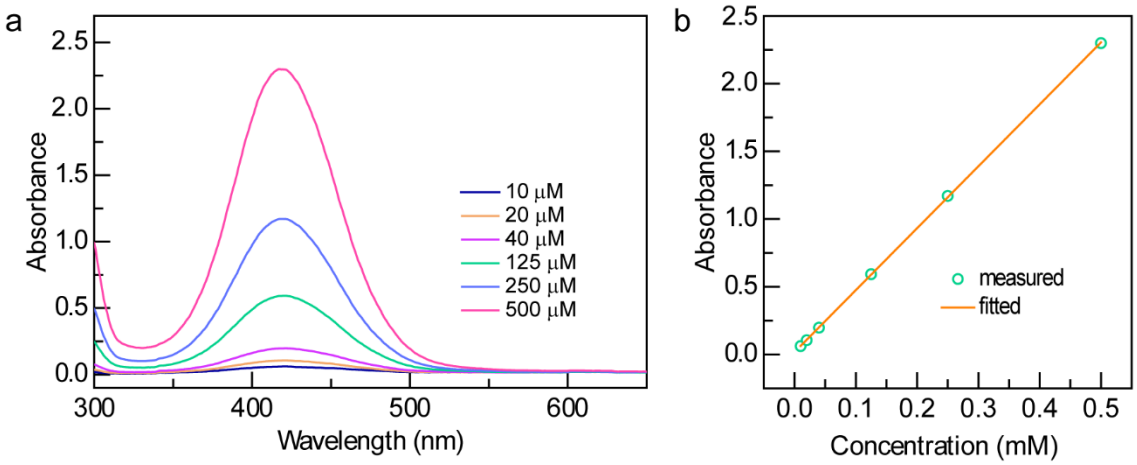

Fig. S17 Calibration relationship for the determination of DAP yield. (a) Absorption spectra of the standard DAP solutions with different concentrations. (b) Linear relationship between the peak absorbance and the concentrations of standard DAP solutions. The fitted linear equation is $y = 4.5729x + 0.01793$. The coefficient of the determination for the linear fitting is R^2 = 0.99995. To calculate the DAP yield, the reaction solution (1 mL) was taken out and centrifuged to remove the catalyst. The value of y is determined by

measuring the peak absorbance of the supernatant, and the value of x is therefore obtained. The DAP yield can be calculated as $\left(\frac{2x}{c_0}\right)$ %, where c_0 is the initial concentration of OPDA.

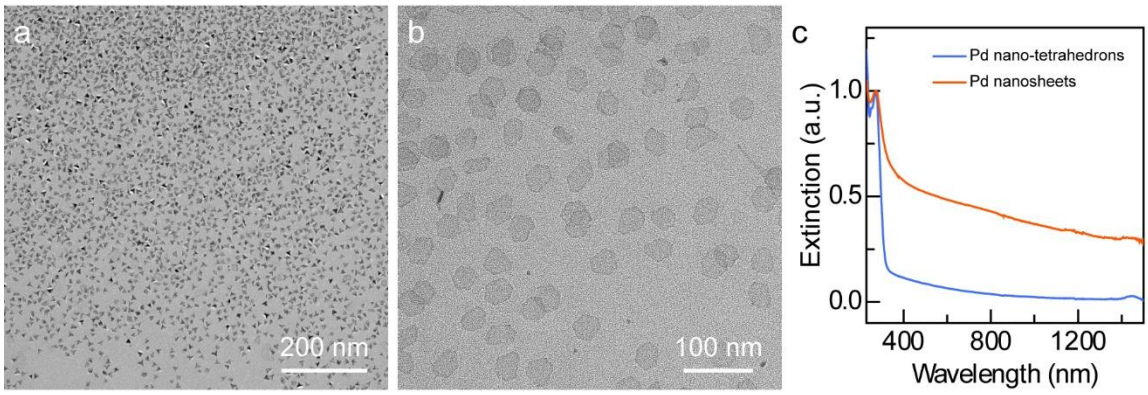

Fig. S18 Samples used for the photothermal experiment. (a, b) TEM images of the Pd nano-tetrahedrons (a) and Pd nanosheets (b). (c) Extinction spectra of the Pd nano-tetrahedrons and Pd nanosheets.

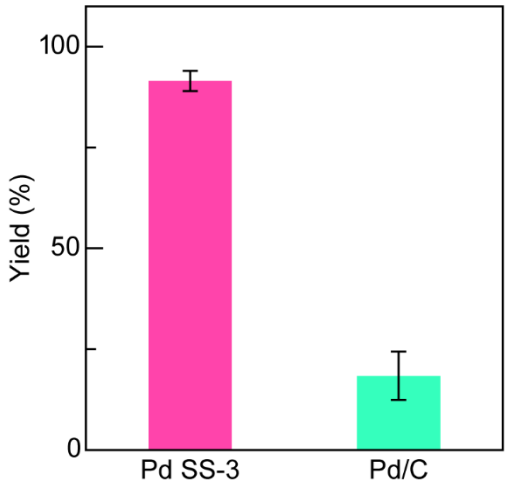

Fig. S19 Photocatalytic activity comparison of the Pd SS-3 sample with the commercial Pd/C catalyst.

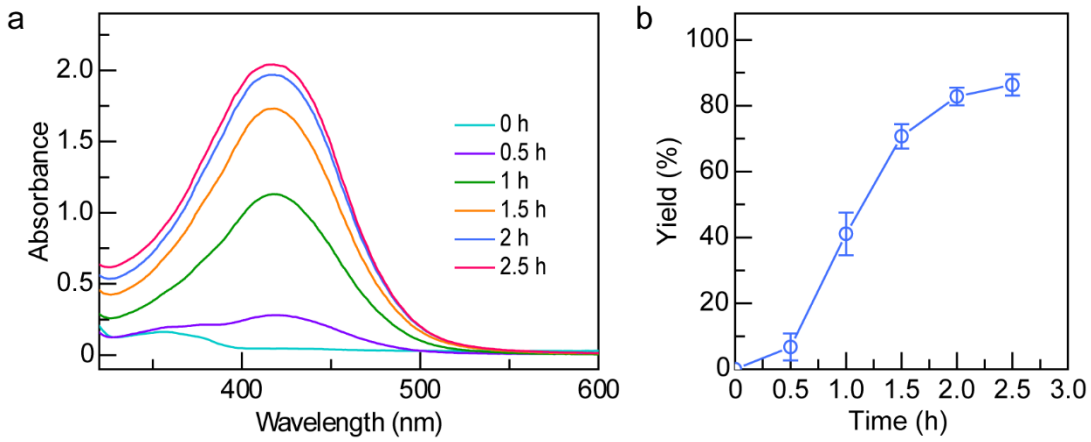

Fig. S20 Time-dependent photocatalytic activity with the Pd SS-3 sample as the catalyst. (a) Absorption spectra of the reaction solutions at different reaction times. (b) Yield of DAP as a function of the reaction time.

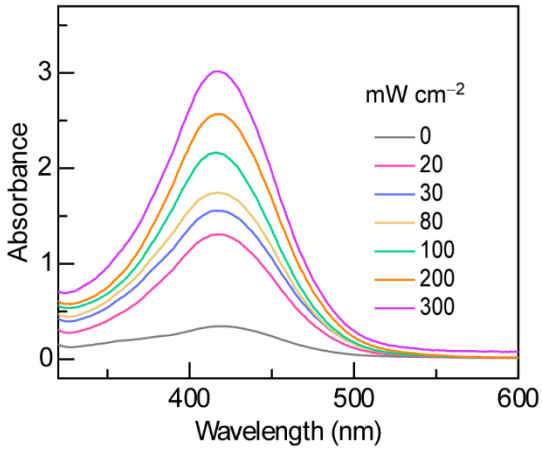

Fig. S21 Optical intensity-dependent absorption spectra with the Pd SS-3 sample as the catalyst.

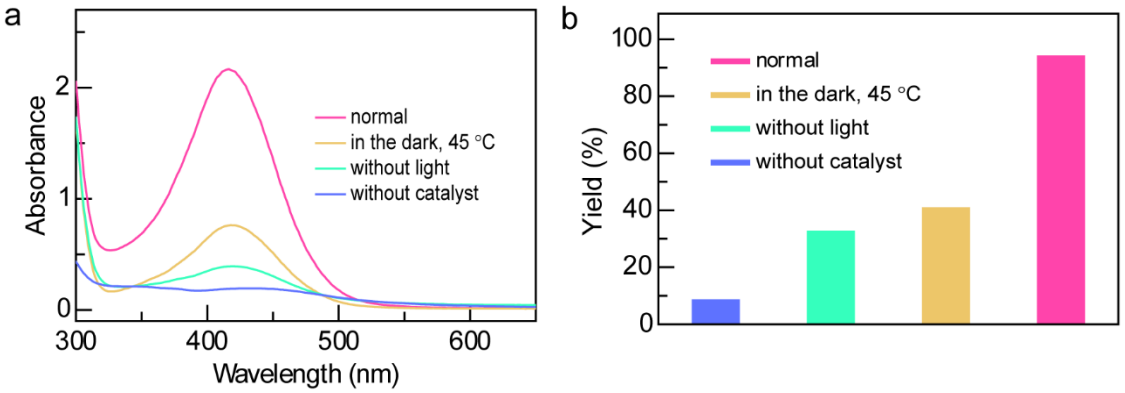

Fig. S22 Control experiments. (a) Absorption spectra of the reaction solutions for performing the photocatalytic experiments under normal condition (red), in 45 °C oil bath in the dark (yellow), without light (green), and without catalyst (blue), respectively. (b) Comparison of the DAP yields under different conditions shown in (a).

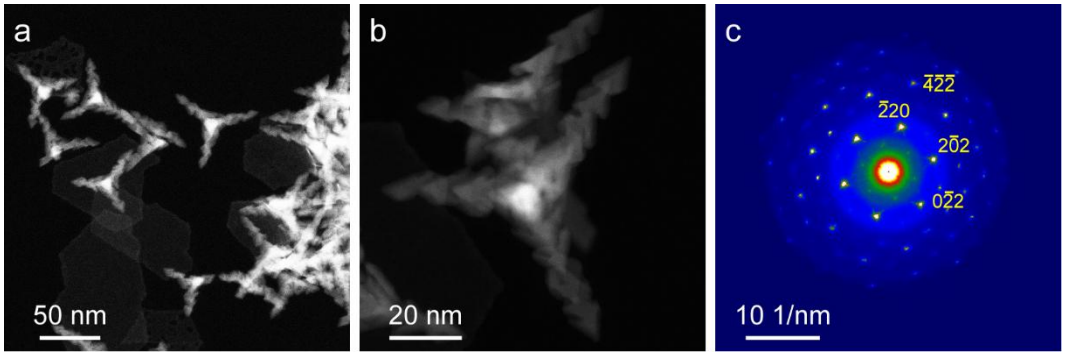

Fig. S23 Stability test. (a, b) Low-(a) and high-magnification (b) STEM images of Pd SSs after the photocatalytic reaction. (c) SAED patterns of the Pd SSs after the photocatalytic reaction.

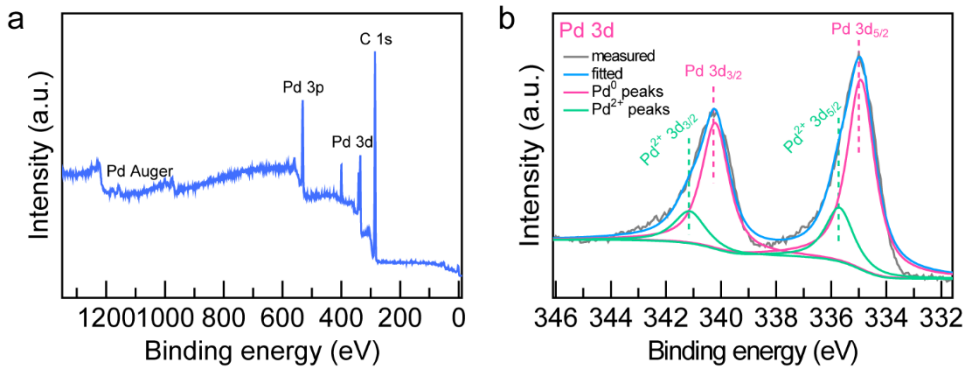

Fig. S24 XPS spectra of the Pd SSs after the photocatalytic test. (a) Survey spectrum. (b) High-resolution Pd 3d spectra.

References

1. X. Q. Huang, S. H. Tang, X. L. Mu, Y. Dai, G. X. Chen, Z. Y. Zhou, F. X. Ruan, Z. L. Yang and N. F. Zheng, *Nat. Nanotechnol.*, 2011, **6**, 28−32.

2. Y. Y. Yang, H. L. Jia, S. H. Su, Y. D. Zhang, M. X. Zhao, J. Z. Li, Q. F. Ruan and C.-y. Zhang, *Chem. Sci.*, 2023, **14**, 10953−10961.